Physical-Parameter Identification of Mid-Story Isolation Buildings Using Backbone Curves

運用背骨曲線於中間樓層隔震建築物之物理參數識別

Ming-Chih Huang[1,*]　Jer-Rong Chang[2]　Chung-Wei Yeh[3]　Jih-Join Shieh[4]
黃銘智[1]　張哲榮[2]　葉崇偉[3]　謝季君[4]
[1,3]Department of Aircraft Engineering, Air Force Institute of Technology
[2]Department of Mechanical Engineering, Air Force Institute of Technology
[4]Center for General Education, Air Force Institute of Technology

[1,3]空軍航空技術學院飛機工程系
[2]空軍航空技術學院機械工程科
[4]空軍航空技術學院通識中心

Abstract

In this research, a physical identification procedure is developed to investigate the dynamic characteristics of a mid-story isolation building equipped with lead-rubber-bearings (LRBs). The primary structure is assumed to be linear on account of substantial reduction of seismic forces due to the installation of LRBs for which a bilinear hysteretic model is considered. The hysteretic model is in turn characterized by a backbone curve by which the multi-valued restoring force is transformed into a single-valued function. With the introduction of backbone curves, the system identification analysis of inelastic structures is significantly simplified. The proposed algorithm extracts individually the physical parameters of each floor of the primary structure and isolation device that are considered useful information in the structural health monitoring. A numerical example is conducted to demonstrate the feasibility of using the proposed technique for physical parameter identification of partially inelastic mid-story buildings

Keywords：Mid-story isolation building, Physical-parameter identification, Backbone curves, Bilinear hysteretic model, Structural health monitoring.

摘要

本研究旨在發展一物理識別過程以識別出中間樓層使用鉛心橡皮支承墊隔震建築物之動態特性。主結構體之動態反應由於鉛心橡皮支承墊的吸能效果將大幅降低，故可假設為線性，而鉛心橡皮支承墊之動態行為則以雙線性遲滯模型模擬之。此遲滯模型將以背骨曲線反映其特徵，藉此原為多值函數之回復力將轉換成單值函數，如此將可大幅簡化非彈性結構之系統識別分析。本文所提之識別過程，可識別出主結構體每一樓層與隔震裝置之物理參數，這些參數對結構健康監測將提供相當有用之訊息。最後藉由數值範例分析，說明本文所提之方法對部分非彈性中間層隔震建築物理參數識別的可行性。

關鍵字：中間樓層隔震建築物、物理參數識別、背骨曲線、雙線性遲滯模型、結構健康監測

1. Introduction

Seismic base isolation is an effective means of damage-proof of building structures against strong earthquakes. The idea of base isolation is to lengthen the fundamental period of the structures so as to avoid resonance with the predominant frequency contents of the earthquakes. Thus, the seismic responses of a base-isolated building can be significantly reduced in comparison with its non-isolated counterpart. Various base isolation systems have been extensively studied both analytically and experimentally since the early 1970s [1-7], and they have been widely adopted all over the world nowadays. Among others, the lead-rubber bearing (LRB) has been the most popular base isolation system adopted for practical implementation in New Zealand, Japan, the United States, Italy, China, and Taiwan [8-10]. Recently, the base isolation technique has been considered even for earthquake protection of tall buildings such as the 32-story Los Angeles City Halls, 18-story Oakland City Hall, and numerous other projects in Japan [11, 12]. Over the last decade, design guidelines and codes with the ordinances of base isolated buildings have been developed for engineering practice. They include the Uniform Building Code (UBC), International Building Code (IBC) and China Design Code for Aseismic Buildings (CDCAB) [13-15].

System identification methods are adopted to estimate structural parameters, including isolation system, according to the recorded responses of the structures with or without input disturbance information. Although various dynamic testing methods have been developed for system identification purposes, it is not practical to identify the system parameters of a massive civil engineering structure through artificial loading tests of any form. However, seismic structural responses recorded during earthquakes provide insight at a modest cost into the structural behavior and dynamic characteristics of targets. Nagarajaiah and Sun [16] investigated the seismic performance of a base-isolated hospital building on the campus of the University of Southern California (USC). Using a bilinear model to represent the base isolation system, their study indicated that the identified responses exhibited favorable agreement with the observed data. The seismic isolation performance of the Fire Command and Control (FCC) building in Los Angeles was further explored by Nagarajaiah and Sun [17]. To characterize the dynamic properties of structural systems under impact loading, a two-dimensional analytical model with an impact spring-dashpot was proposed. Moreover, a three-degree-of-freedom analytical model accounting for the effects of eccentric impact loading was also developed to estimate the parameters of a torsion-coupling (TC) base-isolated building. The parameters identified from the seismic responses were closely related to the analytical model. Accordingly, the seismic performance of the base-isolated FCC building during the Northridge earthquake was proved to be satisfactory. Nagarajaiah and Dharap [18] also developed a new approach for the system identification of base-isolated buildings. A least-squares technique with time segments was proposed for the identification of piecewise linear systems. A series of equivalent linear system parameters was identified from segment to segment. A reduced-order observer was employed in the absence of full-state measurements to estimate the unmeasured states and initial conditions at each time segment. The evolving equivalent linear dynamic properties of the USC hospital building during the Northridge earthquake were determined using the proposed technique. The changes in system parameters, such as the frequencies and damping ratios, caused by the inelastic behavior of the LRBs were reliably estimated. Nagarajaiah and Li [19] conducted a system identification of the FCC building by using the same technique. Huang *et al.* [20] introduced a bilinear backbone curve to represent the pre-yielding and post-yielding stiffness of the isolators, thus converting the complex nonlinear problem into a piecewise linear one. Wang *et al.* [21] assessed the damage of the seismic isolators of the TC structures with various damage indices. The results showed that the proposed indices are capable of localizing damaged isolators.

In this paper, a simplified system identification process is developed to investigate the dynamic characteristics of a mid-story isolation building equipped with lead-rubber-bearings (LRBs). The superstructure and substructure are assumed to be linear on account of substantial reduction of seismic forces due to the installation of LRBs for which a bilinear hysteretic model is considered. The hysteretic model is in turn characterized by a backbone curve by which the multi-valued restoring force is transformed into a single-valued function. With the introduction of backbone curves, the system identification analysis of inelastic structures is simplified to a large extent. The proposed algorithm extracts individually the physical parameters of each floor and the isolation layer that are considered useful information in the structural health monitoring. A numerical example is conducted to demonstrate the feasibility of using the proposed technique for physical parameter identification of partially inelastic mid-story isolation buildings.

2. Motion Equation

Consider a linear multistory shear type structure is installed an isolation layer with lead-rubber bearings (LRBs) between the $i-1$-th and $i+1$-th floors, as shown in Fig.1. The superstructure and substructure are assumed to be linear on account of the reduction in seismic forces due to the installation of isolation layer. Accordingly, the system equation of motion can be expressed as

(a) Superstructure:

$$m_N \ddot{x}_N - R_N(\dot{x}_N - \dot{x}_{N-1}, x_N - x_{N-1}) = -m_N \ddot{x}_g \quad (1)$$

$$m_j \ddot{x}_j + R_j(\dot{x}_j - \dot{x}_{j-1}, x_j - x_{j-1}) - R_{j+1}(\dot{x}_{j+1} - \dot{x}_j, x_{j+1} - x_j) = -m_j \ddot{x}_g$$

$$j = i+1 \sim N-1 \quad (2)$$

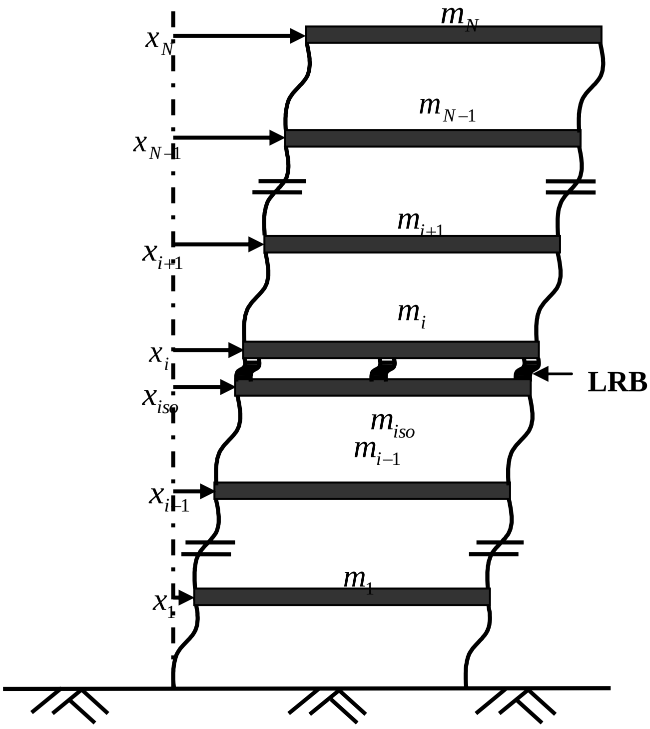

Fig.1 Mid-story isolation building

(b)Isolation layer

$$m_i \ddot{x}_i + r_{iso}(\dot{x}_i - \dot{x}_{iso}, x_i - x_{iso}) - R_{i+1}(\dot{x}_{i+1} - \dot{x}_i, x_{i+1} - x_i) = -m_i \ddot{x}_g \quad (3)$$

$$m_{iso} \ddot{x}_{iso} + R_i(\dot{x}_{iso} - \dot{x}_{i-1}, x_{iso} - x_{i-1}) - r_{iso}(\dot{x}_i - \dot{x}_{iso}, x_i - x_{iso}) = -m_{iso} \ddot{x}_g \quad (4)$$

(c)Substructure

$$m_j \ddot{x}_j + R_j(x_j - x_{j-1}) - R_{j+1}(x_{j+1} - x_j) = -m_j \ddot{x}_g$$

$$j = 2 \sim i-1 \quad (5)$$

$$m_1 \ddot{x}_1 + R_1(\dot{x}_1, x_1) - R_2(\dot{x}_2 - \dot{x}_1, x_2 - x_1) = m_1 \ddot{x}_g$$

$$(6)$$

in which m_j , x_j and R_j are the mass, displacement and restoring force of the j-th floor, respectively; m_{iso} , x_{iso} and r_{iso} are the mass, displacement and restoring force of the isolation layer; and $\ddot{x}_g$ is the ground acceleration. The restoring forces of the superstructure and basement are respectively written as

$$R_j(\dot{x}_j - \dot{x}_{j-1}, x_j - x_{j-1}) = C_j(\dot{x}_j - \dot{x}_{j-1}) + K_j(x_j - x_{j-1})$$

$$j = 2 \sim i-1 \text{ and } j = i+1 \sim N-1 \quad (7)$$

$$R_1(\dot{x}_1, x_1) = C_1(\dot{x}_1) + K_1(x_1) \quad (8)$$

$$r_{iso}(\dot{x}_i - \dot{x}_{iso}, x_i - x_{iso}) = c_{iso}(\dot{x}_i - \dot{x}_{iso}) + h_{iso}(x_i - x_{iso}) \quad (9)$$

where C_j and K_j represent the damping coefficient and stiffness of columns of the j-th floor, respectively, while c_{iso} is the coefficient of viscous damping and h_{iso} is a nonlinear function to be defined later.

3. Bilinear Hysteretic Model

The relation between h_{iso} and the displacement depends on the displacement history. In general, all hysteresis loops are smooth except at the turning points. They can usually be characterized by skeleton curves (backbone curves). Under steady-state cyclic loadings, the hysteretic behavior for these models can be properly described using the criterion attributed to Masing. Masing criterion assumes that the unloading and reloading portion of a hysteresis loop take the same shape as the skeleton curve but with the scale expanded by a factor of two and the origin translated to the point of force reversal [22], as shown in Fig.2. The restoring force is a multi-valued function. However, it is mapped into a single-valued function through the application of skeleton curve. When a hysteretic structure is subjected to transient or cyclic loadings, rules such as those suggested by Jennings or Iwan can be employed to construct the hysteretic loops based on a chosen skeleton curve [22,23].

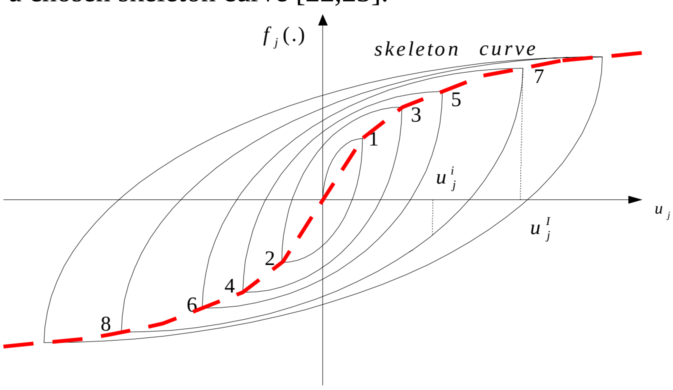

Fig.2 Hysteresis loops based on skeleton loading curve

The restoring force is discretized and expressed, after the first unloading, as

$$h_{iso}(x_i^i - x_{iso}^i) = h_b(x_i^I - x_{iso}^I) + 2 f_{iso}\left(\frac{(x_i^i - x_{iso}^i) - (x_i^I - x_{iso}^I)}{2}\right) \quad (10)$$

in which I is the instant of most recent loading reversal, x_i^i and x_{iso}^i are the displacement of i th-floor and isolation layer, respectively, at instant i with $i = I, I+1, \ldots\ldots\ldots$ and $f_{iso}(\bullet)$ is a function representing the skeleton curve which is assumed to be bilinear in this study.

When Eqs. (7)、(9) and (13) are substituted into Eq.(4), the governing equation of the isolation layer at instant i becomes

$$\begin{aligned} & m_{iso}(\ddot{x}_i^i - \ddot{x}_{iso}^i) + c_{iso}(\dot{x}_i^i - \dot{x}_{iso}^i) + h_{iso}(x_i^I - x_{iso}^I) \\ & + 2 f_{iso}\left(\frac{(x_i^i - x_{iso}^i) - (x_i^I - x_{iso}^I)}{2}\right) \\ & - C_i(\dot{x}_{iso}^i - \dot{x}_{i-1}^i) - K_i(x_{iso}^i - x_{i-1}^i) = m_{iso}(\ddot{x}_g^i + \ddot{x}_i^i) \end{aligned} \quad (11)$$

At instant $i = I$, the above equation becomes

$$\begin{aligned} h_{iso}\left(x_i^I - x_{iso}^I\right) = & -m_{iso}(\ddot{x}_{iso}^I - \ddot{x}_{i-1}^I) - c_{iso}(\dot{x}_i^I - \dot{x}_{iso}^I) \\ & + C_i(\dot{x}_{iso}^I - \dot{x}_{i-1}^I) + K_i(x_{iso}^I - x_i^I) + m_{iso}(\ddot{x}_g^I + \ddot{x}_i^I) \end{aligned} \quad (12)$$

When Eq.(12) is substituted into Eq. (11) , it yields

$$\begin{aligned} & m_{iso}\left[(\ddot{x}_i^i - \ddot{x}_{iso}^i) - (\ddot{x}_i^I - \ddot{x}_{iso}^I)\right] \\ & + c_{iso}\left[(\dot{x}_i^i - \dot{x}_{iso}^i) - (\dot{x}_i^I - \dot{x}_{iso}^I)\right] \\ & + 2 f_{iso}\left[\frac{(x_i^i - x_{iso}^i) - (x_i^I - x_{iso}^I)}{2}\right] \\ & - C_i\left[(\dot{x}_{iso}^i - \dot{x}_{i-1}^i) - (\dot{x}_{iso}^I - \dot{x}_{i-1}^I)\right] \\ & - K_i\left[(x_{iso}^i - x_{i-1}^i) - (x_{iso}^I - x_{i-1}^I)\right] \\ & = m_{iso}\left[(\ddot{x}_g^i + \ddot{x}_i^i) - (\ddot{x}_g^I + \ddot{x}_i^I)\right] \end{aligned} \quad (13)$$

The skeleton curve is characterized by three line segments with slopes of k_{isoe} or k_{isoy} as

$$\begin{aligned} f_{iso}(v) &= k_{isoe} v & -D \le v \le D \\ &= b_{iso} + k_{isoy} v & v > D \\ &= -b_{iso} + k_{isoy} v & v < -D \end{aligned} \quad (14)$$

where D denotes the yielding displacement and b_{iso} the characteristic strength. When Eq. (14) is substituted into Eq. (13) , the governing equation can be rewritten as

$$\ddot{u}_{iso}^i + \frac{c_{iso}}{m_{iso}}\dot{u}_{iso}^i + \frac{k_{isoe}}{m_{iso}}u_{iso}^i = \ddot{u}_g^i \qquad -D \le u_{iso} \le D \quad (15)$$

$$\ddot{u}_{iso}^i + \frac{c_{iso}}{m_{iso}}\dot{u}_{iso}^i + \frac{2b_{iso}}{m_{iso}} + \frac{2k_{isoy}}{m_{iso}}u_{iso}^i = \ddot{u}_g^i \qquad u_{iso} > D \quad (16)$$

$$\ddot{u}_{iso}^i + \frac{c_{iso}}{m_{iso}}\dot{u}_{iso}^i - \frac{2b_{iso}}{m_{iso}} + \frac{k_{isoy}}{m_{iso}}u_b^i = \ddot{u}_g^i \qquad u_{iso} < -D \quad (17)$$

where

$$u_{iso}^{i} = \left[(x_i^i - x_{iso}^i) - (x_i^I - x_{iso}^I) \right] \qquad (18)$$

$$\ddot{u}_g^i = \left[(\ddot{x}_g^i + \ddot{x}_i^i) - (\ddot{x}_g^I + \ddot{x}_i^I) \right] + \frac{C_i}{m_{iso}}[(\dot{x}_{iso}^i - \dot{x}_{i-1}^i) - (\dot{x}_{iso}^I - \dot{x}_{i-1}^I)] + \frac{K_i}{m_{iso}}[(x_{iso}^i - x_{i-1}^i) - (x_{iso}^I - x_{i-1}^I)] \qquad (19)$$

Equations (15)~(17) are used to identify the parameters of the isolation layer.

Similarly, substituting Eqs.(4) (i.e. $r_{iso}(\dot{x}_i - \dot{x}_{iso}, x_i - x_{iso}) = m_{iso}(\ddot{x}_{iso} + \ddot{x}_g) + R_i(\dot{x}_{iso} - \dot{x}_{i-1}, x_{iso} - x_{i-1})$), (7) and (9) into Eq.(3), we obtain the equation for identifying the damping coefficient and stiffness of the i+1-th floor as

$$\ddot{x}_i - \frac{C_{i+1}}{m_i}(\dot{x}_{i+1} - \dot{x}_i) - \frac{K_{i+1}}{m_i}(x_{i+1} - x_i) = -\ddot{x}_g - \frac{m_{iso}}{m_i}(\ddot{x}_{iso} + \ddot{x}_g) - \frac{C_i}{m_i}\left(\dot{x}_{iso} - \dot{x}_{i-1}\right) - \frac{K_i}{m_i}(x_{iso} - x_{i-1}) \qquad (20)$$

and the error function for the $i+1$-th floor is defined as

$$e_{fi+1} = \sum_{i=1} \left[\begin{array}{l} \ddot{x}_i + \frac{C_i}{m_i}\left(\dot{x}_{iso} - \dot{x}_{i-1}\right) + \frac{K_i}{m_i}(x_{iso} - x_{i-1}) \\ - \frac{C_{i+1}}{m_i}(\dot{x}_{i+1} - \dot{x}_i) - \frac{K_{i+1}}{m_i}(x_{i+1} - x_i) \\ + \ddot{x}_g + \frac{m_{iso}}{m_i}(\ddot{x}_{iso} + \ddot{x}_g) \end{array} \right]^2 \qquad (21)$$

Extremization of Eq.(21) with respect to the unknowns yields

$$\frac{\partial e_{fi+1}}{\partial \left(C_{i+1} / m_i \right)} = 0 \qquad \frac{\partial e_{fi+1}}{\partial \left(K_{i+1} / m_i \right)} = 0 \qquad (22)$$

With C_i and K_i derived already from the previous step, C_{i+1} and K_{i+1} are obtained by solving Eq.(22) simultaneously for $j = i + 1 \sim N$.

4. Numerical Example

As an illustration to verify the proposed methodology for system identification of mid-story isolation buildings, a numerical example is considered using a 3-story shear building with a plane of $10m \times 10m$ and story height of 3m. The isolation layer consists of five LRB bearings, which locates between floor 1 and floor 2. The system parameters considered in the study include: (1) $m_1 = m_2 = m_3 = 58.32 \times 10^3 kg$ and $K_1 = K_2 = K_3 = 168.06 MN/m$ for the superstructure and substructure ; (2) $m_{iso} = 68.04 \times 10^3 kg$, $b_{iso} = 245.25 kN$, $k_{isoe} = 44.145 MN/m$, and

$k_{isoy} = 6.867\,MN/m$ for the isolation layer and LRB.

Dynamic responses of the mid-story isolation building under the N-S component of the 1940 El Centro earthquake are calculated using Newmark's linear acceleration method with a time-step of 0.02sec. The acceleration responses contaminated with an artificial white noise signal of 5% noise-to-signal ratio are considered in the system identification analysis to simulate the measured data in a more realistic manner.

Fig. 3 presents the nonlinear restoring force of isolation layer (LRBs) with a yielding displacement of 0.658 cm and a ductility ratio of 7.322. The force-displacement relationship of the story shear at the first floor and third floor are almost linear, as illustrated in Figs. 4 and 5.

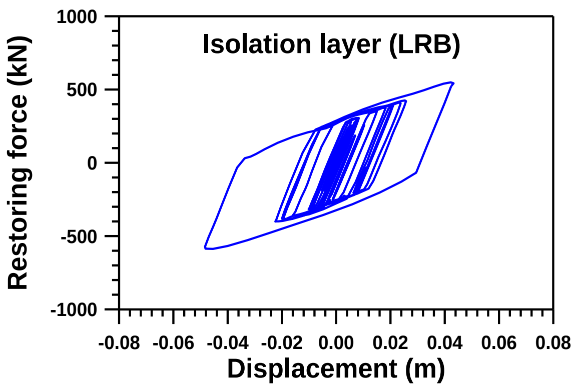

Fig.3 Nonlinear restoring force of isolation layer

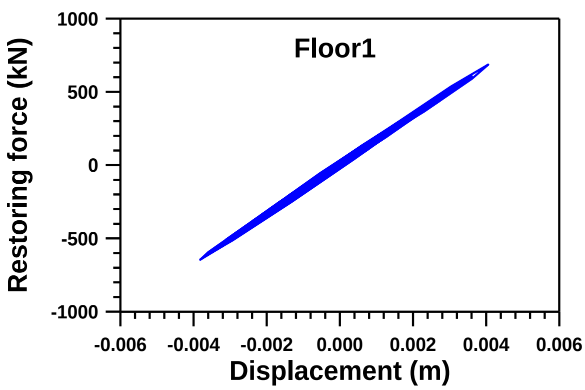

Fig.4 Restoring force and displacement of floor1

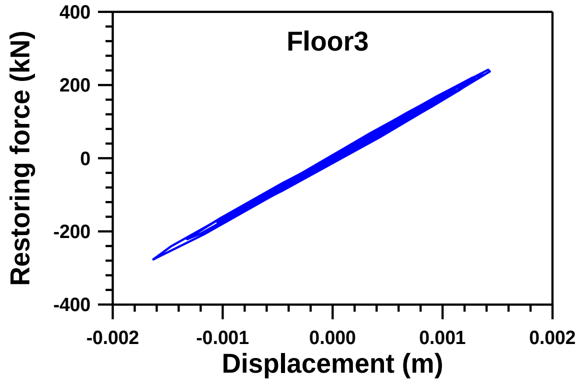

Fig.5 Restoring force and displacement of floor3

In the first cycle of identification, the initial value of C_1 is set to be zero arbitrarily. The global measure-of-fit as a function of K_1 is presented in Fig. 6, which reveals that the least squares estimate of K_1 is $160MN/m$. Then K_1 is fixed at this value and the minimization process is performed. As illustrated in Fig. 7, the optimal estimate of C_1 is $250kN.s/m$. In the meantime, the identified parameter values of isolation layer are $c_{iso} = 134kN.s/m$, $b_{iso} = 236.44kN$, $k_{isoe} = 42.606MN/m, k_{isoy} = 6.656\,MN/m$. Then, substituting $C_1 = 250kN.s/m$ and $K_1 = 160MN/m$ into Eq.(20) through the minimization process, the identified parameter values of floor2 are $C_2 = 225kN.s/m$ and $K_2 = 161.92MN/m$. Finally, the parameters of the 3-th floor can be obtained in a similar manner. Application of the Eqs.(2) and (7) identified parameter values of floor3, the optimal estimate of C_3 and K_3 are $C_3 = 178kN.s/m$ and $K_3 = 159.94MN/m$, respectively. We call this constitutes is one cycle of identification.

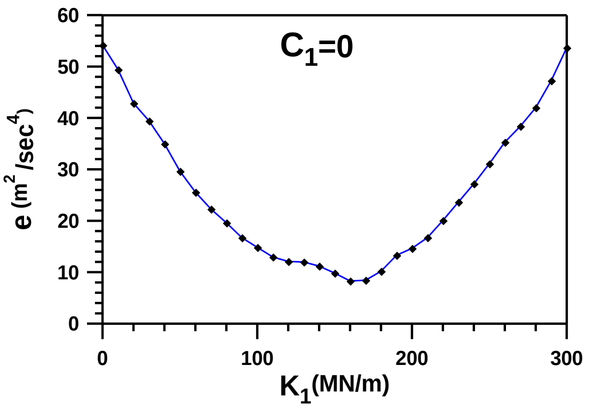

Fig.6 Global measure-of-fit in the first cycle setting $C_1 = 0kN.s/m$

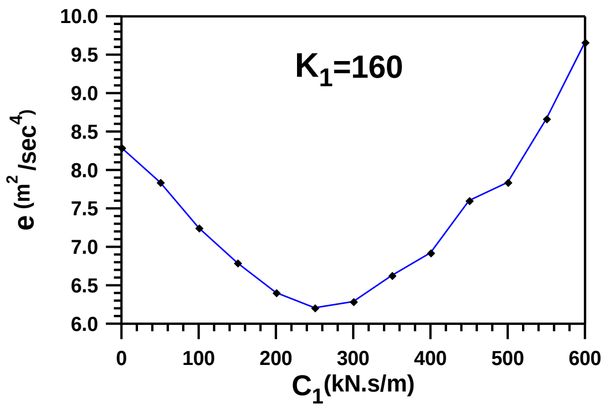

Fig.7 Global measure-of-fit in the first cycle setting $K_1 = 160MN/m$

The second identification cycle is then proceeded. The initial value of C_1 is equal to $250kN.s/m$. Minimizing the global measure-of-fit, we have $K_1 = 165MN/m$, Fig. 8. Numerical calculation suggests that three cycles of identification are sufficient. Column 2~5 and column 6~7 in Table 1, respectively summarize the iterative identified parameter values of isolation layer and first floor. Similarly, columns 2~5 in Table 2 list the identified parameters of floor2 and floor3. In addition, the identified skeleton curve (backbone curve) of isolation layer is drawn in Fig. 9. It clearly indicates the application of Masing criterion.

Table 1 Identified parameter of floor1 and isolation layer

1	2	3	4	5
Number of cycle	c_{iso} $kN.s/m$	b_{iso} kN	k_{isoy} MN/m	k_{isoe} MN/m
1	134	236.44	6.656	42.606
2	143	242.07	6.795	43.716
3	144	242.67	6.808	43.822
True Value	146	245.25	6.867	44.145
EI	0.1144			
1	6		7	
Number of cycle	C_1 $kN.s/m$		K_1 MN/m	
1	250		160.00	
2	270		165.00	
3	276		165.50	
True Value	321		168.06	
EI	0.1794			

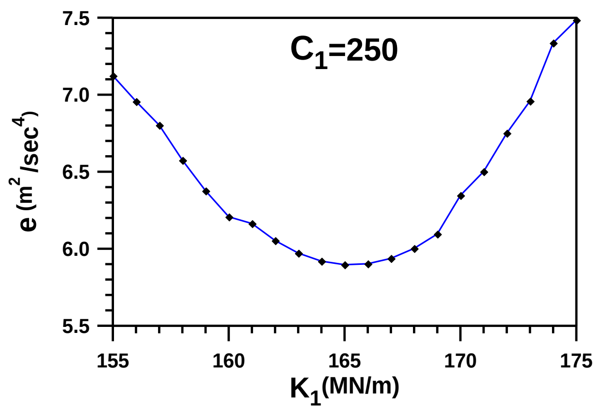

Fig.8 Global measure-of-fit in the second cycle setting $C_1 = 250kN.s/m$

Table 2 Identified parameter of floor 2 and floor 3

1	2	3	4	5
Number of cycle	C_2 $kN.s/m$	K_2 MN/m	C_3 $kN.s/m$	K_3 MN/m
1	225	161.92	178	159.94
2	270	165.65	247	164.64
3	276	166.04	257	165.16
True Value	321	168.06	321	168.06
EI	0.0855		0.1058	

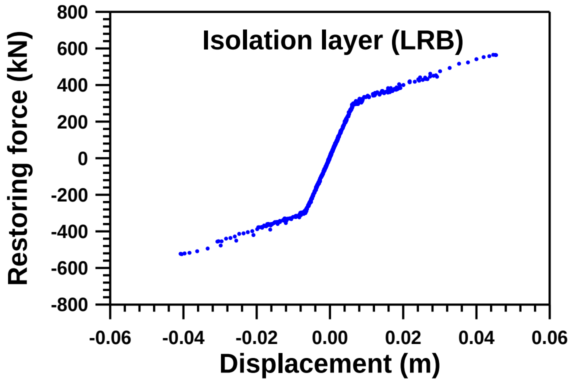

Fig.9 Identified skeleton curve of isolation layer

The comparison between the identified and measured response is made. Figs. 10 and 11 show the acceleration and displacement responses of the floor1, respectively. The identified and measured ones are virtually identical. Similarly, the acceleration and displacement responses of the isolation layer and floor3 are presented in Figs. 12-15, respectively. They also promise an excellent identification.

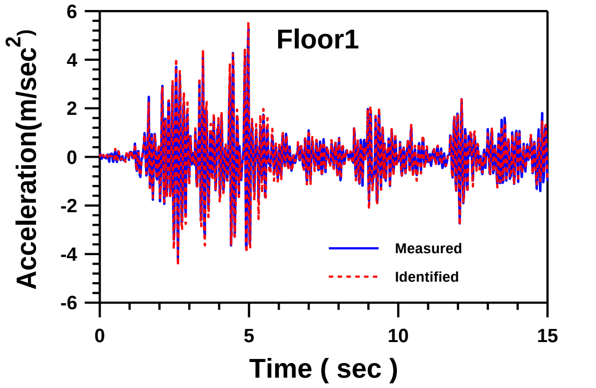

Fig.10 Comparison between identified and measured accelerations of floor 1

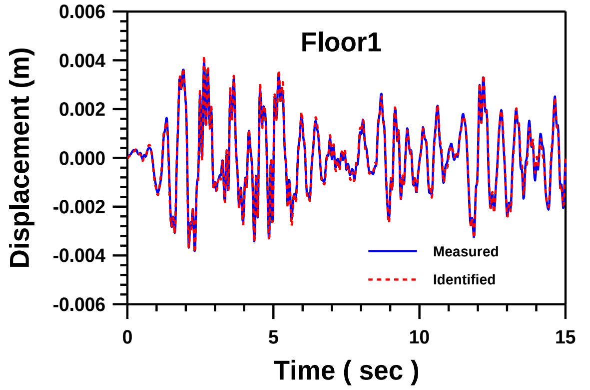

Fig.11 Comparison between identified and measured displacements of floor1

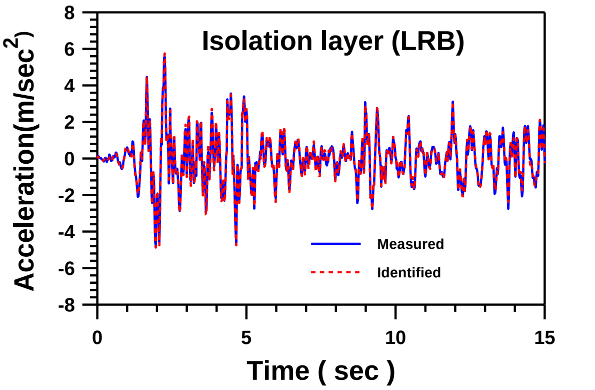

Fig.12 Comparison between identified and measured accelerations of isolation layer

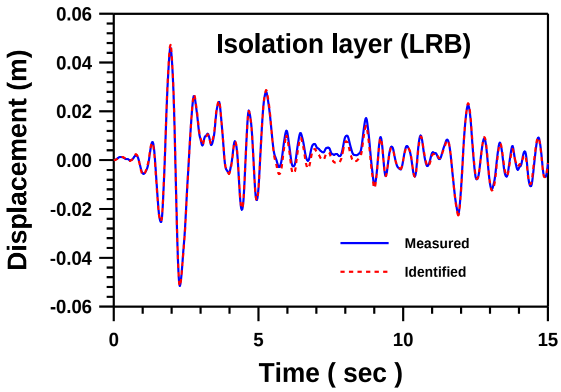

Fig.13 Comparison between identified and measured displacements of isolation layer

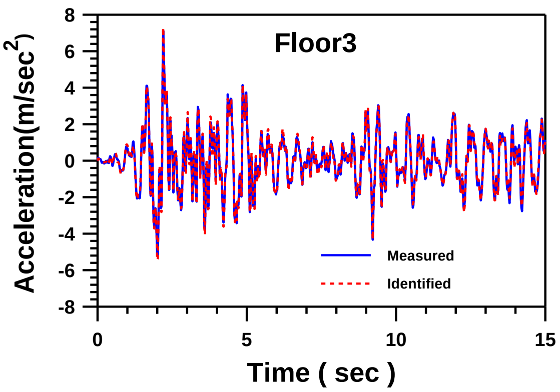

Fig.14 Comparison between identified and measured accelerations of floor 3

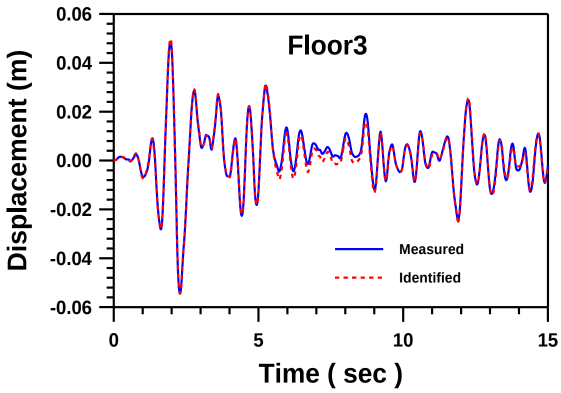

Fig.15 Comparison between identified and measured displacements of floor 3

5. Conclusions

In this paper, a physical identification procedure of mid-story isolation buildings equipped with LRBs is developed. The hysteretic behavior of the nonlinear system is characterized by a backbone curve, by which the multivalued restoring force is transformed into a single-valued function; consequently, the system identification analysis of inelastic structures is greatly simplified. The feasibility of the proposed scheme is demonstrated using the numerical example of a 3-story shear building with isolation layer. Features of the proposed procedure include:

(a) All physical parameters of the isolated system in terms of the bilinear stiffness and damping coefficients can be identified.

(b) The system parameters are identified with reasonable accuracy in three iterations, even in the presence of noise contamination. The robustness of the algorithm makes it a favorable alternative for practical applications.

(c) The proposed algorithm extracts the physical parameters of the system, which reveals the actual behavior of nonlinear systems more than does using modal parameters representing only equivalent linear systems.

References

1. Kelly J. M., “A seismic base isolation: review and bibliography”, Soil Dynamics and Earthquake Engineering, Vol.5, No.3, pp.202-217 (1993).
2. Koh C. G. and Kelly J. M, “Viscoelastic stability model for elastomeric isolation bearings”, Journal of Structural Engineering, ASCE, Vol.115, No.2, pp.285-302 (1989).
3. Fan F. G. and Ahmadi G., “Seismic responses of secondary systems in base-isolated structures”, Engineering Structures, Vol.14, No.1, pp.35-48

(1992).
4. Pan T. C. and Cui W., “Dynamic characteristics of shear buildings on laminated rubber bearings”, Earthquake Engineering and Structural Dynamics, Vol.23, No.12, pp.1315-1329 (1994).
5. Chung W. J., Yun C. B. and Kim N. S., “Shaking table and pseudo-dynamic tests for the evaluation of the seismic performance of base-isolated structures”, Engineering Structures, Vol.21, No.4, pp.365-379 (1999).
6. Huang W. J. and Hsu T. Y., “Experimental study of isolated building under triaxial ground excitations”, Journal of Structural Engineering, ASCE, Vol.126, No.8, pp.879-886 (2000).
7. Jangid R. S. and Kelly J. M., “Base isolation for near fault motions”, Earthquake Engineering and Structural Dynamics, Vol.30, No.5, pp.691-707 (2001).
8. Shinner R. I., Robinson W. H. and McVerry G. H., An introduction to seismic isolation, Wiley, New York (1993).
9. Li H. N. and Wu X. X, “Limitations of height-to-width ratio for base-isolated buildings under earthquake”, The Structural Design of Tall and Special Buildings, Vol.15, pp.277-287 (2006).
10. Lee Z. K., Wu T. H. and Lo C. H., “System identification on the seismic behavior of an isolated bridge”, Earthquake Engineering and Structural Dynamics, Vol.32, pp.1797-1812 (2003)
11. Keri L. R. and Anil K. C., “Estimating seismic demands for isolation bearings with building overturning effects”, Journal of Structural Engineering, ASCE, Vol.123, No.7, pp.1118-1128 (2006).
12. Pan P., Zamfirescu D. Nakayasu M. and Kashiwa H, “Base-isolation design practice in Japan: Introduction to the post-Kobe approach”, Journal of Earthquake Engineering, Vol.9, No.1, pp.147-171 (2005).
13. ICBO (International Conference of Building Officials), Uniform Building Code (UBC), Whitter, CA. (1997)
14. ICC (International Code Council), International Building Code (IBC), final draft. Whitter, CA. (1998)
15. China Standard and Code Committee, China Design Code for Aseismic Buildings (CDCAB), China building Industrial Press, Beijing. (2000)
16. Nagarajaiah S., Sun X., “Response of base-isolated USC hospital building in Northridge earthquake”, Journal of Structural Engineering, ASCE, Vol.126, No.10, pp.1177-1186 (2000).
17. Nagarajaiah S., Sun X., “Base-isolated FCC building: impact response in Northridge earthquake”, Journal of Structural Engineering, ASCE, Vol.127, No.9, pp.1063-1075 (2001).
18. Nagarajaiah S., Dharap P., “Reduced order observer based identification of base isolated buildings”, Earthquake Engineering and Engineering Vibration, Vol.2, No.2, pp.237-244 (2003).
19. Nagarajaiah S., Li Z., “Time segmented least squares identification of base isolated buildings”, Soil Dynamics and Earthquake Engineering, Vol.24, pp.577-586 (2004).
20. Huang M. C., Wang Y. P., Chang J. R., Chen Y. H., “Physical-parameter identification of base-isolated buildings using backbone curves”, Journal of Structural Engineering, ASCE, Vol.135, No. 9, pp.1107-1114 (2009).
21. Wang J. F., Huang M. C., Lin C. C., Lin T. K.,

"Damage identification of isolators in base-isolated torsionally coupled buildings", International Journal of Smart Structures and Systems, Vol.11, No.4, pp.387-410 (2013).

22. Jennings P. C., "Earthquake response of yielding structure", *Journal of Engineering Mechanics Division*, ASCE, Vol.91, pp.41-68 (1965).

23. Iwan W. D., "On a class of models for the yielding behavior of continuous and composite system", *Journal of Applied Mechanics*, ASCE, Vol.34, pp.612-617 (1967).